BROADBAND SEISMIC STUDIES IN SOUTHERN ASIA

Keith Priestley,[1] Vinod K. Gaur,[2] S. S. Rai,[2] Jessie L. Bonner,[3] and James F. Lewkowicz[3]

Cambridge University,[1]
Center for Mathematical Modeling and Computational Sciences, Bangalore, India[2]
Weston Geophysical Corporation[3]

Sponsored by Defense Threat Reduction Agency

Contract No. DTRA01-00-C-0028

ABSTRACT

We are continuing efforts to develop 3-D velocity models for southern Asia through the collection and analysis of broadband waveform data acquired on the Indian subcontinent. The geology of India is diverse, but can be divided into three main regions: the Himalayas, the Indo-Gangetic plain, and the Indian Shield. Our initial focus has been on the southern Indian shield, and we have also completed studies in the trans-Himalayas and the Shillong Plateau. The goal of our work is to determine the crust and upper mantle velocity and attenuation structure and to characterize regional seismic waveform propagation of the Indian subcontinent. Teleseismic receiver function data, S-to-P conversions, and short-period surface wave phase velocity data have been interpreted for seismograms recorded along a 700-km north-south profile of the southern Shield. These data show that the shield velocity structure is extremely uniform, simple, and consists of a surface wave velocity of approximately 3.45 km/sec and a moderate gradient of 0.20 km/sec/km with the Moho at 35±1 km depth. To the south of the shield in the granulite terrain, the crust is both thicker (44±1 km deep) and more complicated, with a mid-crustal discontinuity at approximately 25-km depth. We constrain the upper mantle structure with phase velocity measurements of long-period surface waves; these show that the seismic lithosphere is approximately 150 km thick and underlain by a weak low-velocity zone. We have also modeled the regional waveforms of a moderate earthquake that occurred near Koyna, India, in September 2000 and of the 26 January 2001 Bhuj main shock and its aftershocks to calibrate paths to the regional stations.

KEY WORDS: waveform modeling, velocity models, surface waves, receiver functions

OBJECTIVES

The objectives of our research effort are fourfold. The first is to increase the amount of high quality seismic data that are available by deploying additional seismic stations in the India/Pakistan region. The second is to use these data to refine the regional attenuation characteristics, the regional travel time corrections, and the crust and upper mantle structure of the region. The third is to use the analysis of these data to refine Weston's 3-D velocity model for India and Pakistan (WINPAK3D) and to validate the model. The fourth is to provide a cooperative forum for the exchange of information and ideas on the analysis of the data and modeling of the region.

This research is motivated by the fact that calibrated regional velocity models for the India/Pakistan region will be essential to improve upon the location capability of global networks. For example, Table 1 lists five earthquakes that occurred in the Koyna-Warna region along the western coast of India. Yet, even with some overlap in the datasets processed by the three institutions, the locations formed by the networks show significant scatter (Figure 1). In fact, of the 15 different locations for the five events, only four locations fall within or near the boundary of the seismicity cluster regions determined for the Koyna-Warna region by Mandal *et al*. (1998). This region is well known for the clustered seismic activity that started in 1962 after the impoundment of the Koyna reservoir. The events were recorded on global seismic networks and located by the Prototype International Data Center (pIDC), United States Geological Survey (USGS), and International Seismic Centre (ISC). In addition to the locations, we present the range of group velocity dispersion curves generated for HYB data (Figure 2) using the event source locations and origin times presented in Table 1. For reference, we have plotted the theoretical dispersion curve generated using our shear wave velocity model for the southern Indian

Report Documentation Page

Form Approved
OMB No. 0704-0188

1. REPORT DATE	2. REPORT TYPE	3. DATES COVERED
OCT 2001		**00-00-2001 to 00-00-2001**

4. TITLE AND SUBTITLE	5a. CONTRACT NUMBER
Broadband Seismic Studies In Southern Asia	5b. GRANT NUMBER
	5c. PROGRAM ELEMENT NUMBER
6. AUTHOR(S)	5d. PROJECT NUMBER
	5e. TASK NUMBER
	5f. WORK UNIT NUMBER
7. PERFORMING ORGANIZATION NAME(S) AND ADDRESS(ES) **Cambridge University,Bullard Labs of The Department of Earth Science,Madingley Rd, Cambridge, CB3 OEZ, UK, ,**	8. PERFORMING ORGANIZATION REPORT NUMBER
9. SPONSORING/MONITORING AGENCY NAME(S) AND ADDRESS(ES)	10. SPONSOR/MONITOR'S ACRONYM(S)
	11. SPONSOR/MONITOR'S REPORT NUMBER(S)

12. DISTRIBUTION/AVAILABILITY STATEMENT
Approved for public release; distribution unlimited

13. SUPPLEMENTARY NOTES
Proceedings of the 23rd Seismic Research Review: Worldwide Monitoring of Nuclear Explosions held in Jackson Hole, WY on 2-5 of October, 2001. U.S. Government or Federal Rights.

14. ABSTRACT
See Report

15. SUBJECT TERMS

16. SECURITY CLASSIFICATION OF:			17. LIMITATION OF ABSTRACT	18. NUMBER OF PAGES	19a. NAME OF RESPONSIBLE PERSON
a. REPORT **unclassified**	b. ABSTRACT **unclassified**	c. THIS PAGE **unclassified**	**Same as Report (SAR)**	**10**	

shield that is discussed later in this paper and presented in Figure 4. Because the path from these events to HYB (Δ - 525 km; azimuth - 90°) is essentially the same for all events in the region, and focal mechanisms for all three clusters are similar (Mandal, *et al*, 1998), differences in the dispersion curves must be related to location and/or origin time errors. The average dispersion curve generated by these data at shorter periods has approximately ± 0.2 seconds error and thus would incorporate considerable error if used to develop a shear wave velocity model for the region. For the model development described in the following sections of this paper, we have searched for and examined only well-located events in order to reduce such model error. The results are high-quality regional velocity models for southern Asia that have been incorporated into WINPAK3D and are being used to more accurately locate regional seismic events in southern Asia.

	pIDC				ISC				USGS			
EVID	OT	Lat	Long	Depth	OT	Lat	Long	Depth	OT	Lat	Long	Depth
19950312	08:22:54.9	17.19	73.58	15	08:22:55.4	17.38	73.91	17.7	08:22:54.69	17.64	73.77	10F
19950313	03:09:47.0	17.20	73.47	15	03:09:37.9	17.41	73.98	16.9	03:09:42.5	17.52	74.12	54
19960426	12:19:34.8	17.09	73.49	17.9	12:19:34.1	17.19	73.72	29.0	12:19:33.4	17.16	73.56	22
19980211	01:08:52.5	17.13	73.76	16	01:08:49.1	17.32	73.96	33F	01:08:49.3	17.16	73.79	33F
19980214	00:59:49.0	17.15	73.66	18	00:59:50.8	17.38	73.87	33F	00:59:51.6	17.25	73.52	33F

Table I. Source parameters from the pIDC, ISC, and USGS for five earthquakes near the Koyna-Warna region of western India.

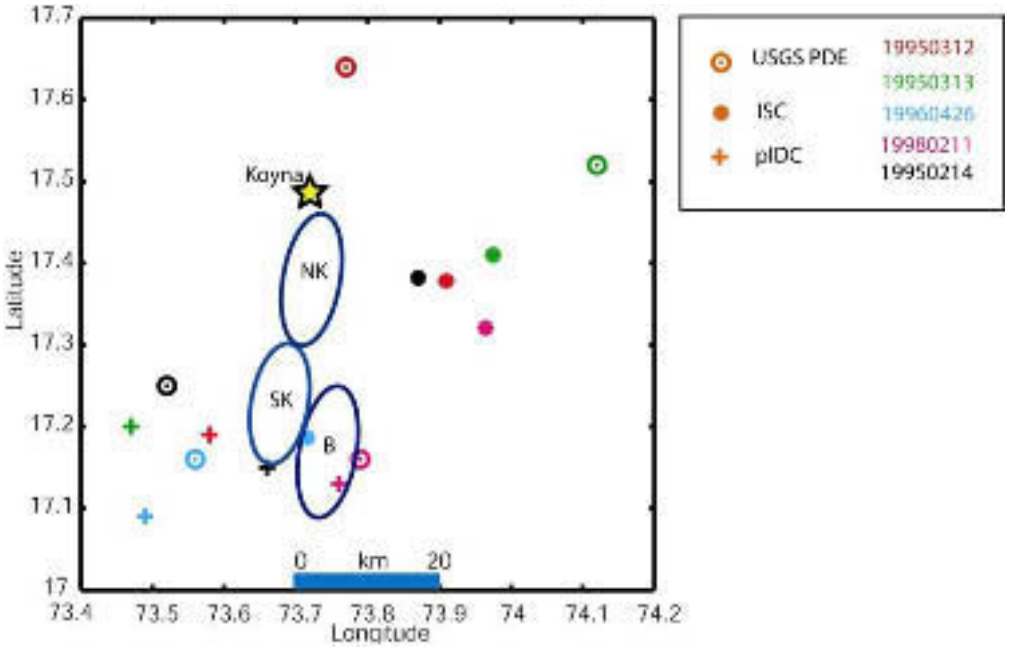

Figure 1. USGS, pIDC, and ISC network locations for the five earthquakes listed in Table 1. The three ellipsoids represent the distinct regions of the Koyna-Warna seismic zone where the majority of the seismicity occurs (Mandal et al., 1998) The abbreviations for each cluster include NK - Northern Koyna; SK - Southern Koyna; and B - Bhogiv.

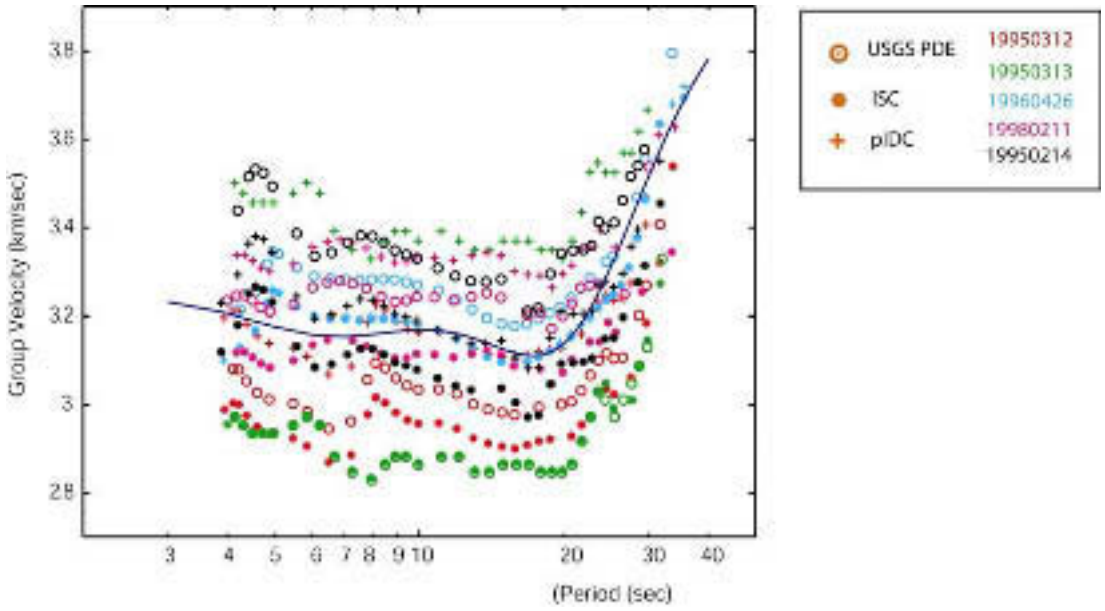

Figure 2. Group velocity dispersion for paths between the Koyna-Warna region and station HYB. The scatter in the dispersion curves is related to location and origin time errors and illustrates the need for using only high-quality event data to generate the calibrated regional velocity models. The blue line is the theoretical dispersion curve for the south Indian shield as determined by research discussed in the following section.

RESEARCH ACCOMPLISHED

Installation of Broadband Seismographs in India

In early February we received five broadband seismographs from Guralp Systems Limited, which we deployed in India in March/April of this year. Figure 3 shows the location of these stations and other stations we are currently operating in India in cooperation with the National Geophysical Research Institute at Hyderabad and the Indian Institute of Astrophysics at Bangalore.

Crustal structure beneath southern India

Short-period surface wave studies. Surface wave phase velocities for fundamental mode Rayleigh waves have been measured for a number of paths across the south Indian Shield (Figure 3). The analysis of surface wave dispersion data gives an average crustal model for the south Indian Shield that is used as a starting model in the receiver function inversions discussed below, and provides additional constraints in the joint receiver function - surface wave inversion.

We determined an average short period fundamental mode Rayleigh wave dispersion curve using various two-station pairs along the North-South (NS) profile using the transfer function method of Gomberg *et al.* (1988). This technique poses the problem of phase velocity determination as a linear filter estimation problem in which the seismogram at a more distant station from an event is the convolution of the seismogram at a close station with the Earth filter (the phase velocity curve) to be determined. Smoothness constraints are imposed based on an approximate knowledge of the group velocity. We used the dispersion results of Bhattacharya (1992) as an initial dispersion model. To ensure the starting dispersion curve was appropriate, we tested a number of initial dispersion models and smoothing criteria; the final dispersion curves (Figure 4a) are the ones where the results were stable in the sense that the resulting dispersion curve

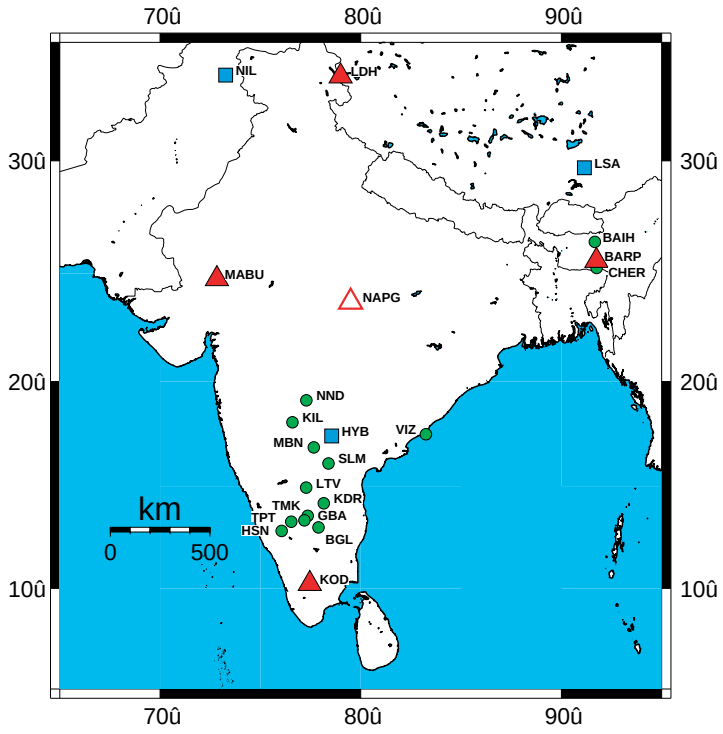

Figure 3. Map showing the stations locations: triangles - permanent stations of Indian Institute of Astrophysics/University of Cambridge; dots - temporary recording sites of National Geophysical Research Institute/University of Cambridge; squares - global digital seismic network stations.

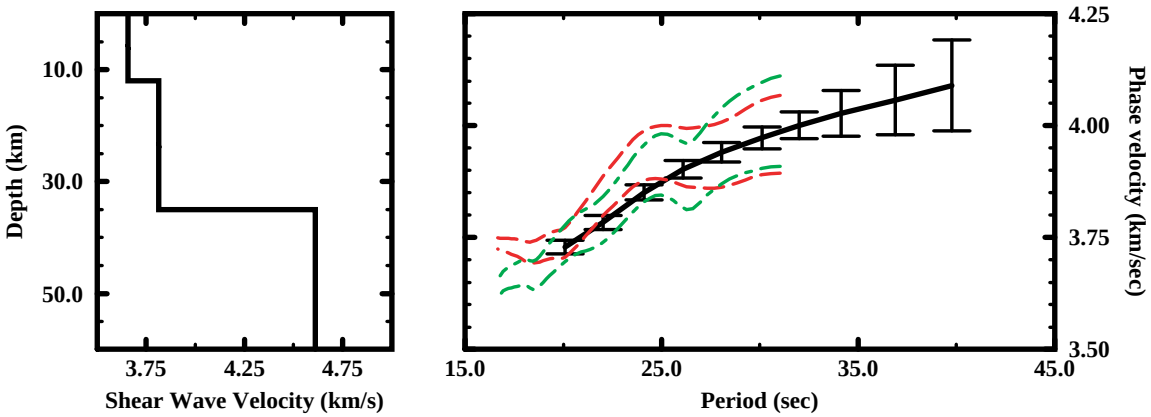

Figure 4. Right - Fundamental mode Rayleigh wave dispersion curves: solid line with error bars - average dispersion for the NS profile; dashed lines - dispersion bounds for the northern portion of NS profile; dot-dash lines - dispersion bounds for the southern portion of NS profile. Left - Crustal velocity model derived from inversion of the average dispersion curve.

was not strongly influenced by realistic changes in the initial dispersion model and smoothing criteria. The dispersion curves in Figure 4a were determined simultaneously from multiple station pairs, but we also determined dispersion curves for all individual two-station paths separately to verify that there were no large outliers amongst the various two-station combinations.

We invert the Rayleigh wave phase velocity data using the stochastic least-squares routine of Hermann (1994). This expresses the standard least-squares problem in terms of eigenvalues and eigenvectors and uses singular value decomposition to invert the matrix giving the solution vector, the variance-covariance matrix, and the resolution matrix. Since the dispersion data for the northern portion, southern portion, and whole profile were nearly identical, and since the crustal models from refraction data at the northern (Krishna *et al*., 1999) and southern (Krishna and Ramesh, 2000) ends of the profile are similar, we inverted only the average dispersion curve. The starting model for the inversion is from the average crustal model for the Indian Shield of Singh *et al*. (1999) and consisted of an upper crustal layer 13.8 km thick with Vs 3.55 km/s and a lower layer 24.9 km thick with Vs 3.85 km/s, over a 4.65 km/s half-space. The final inversion model and the fit of the dispersion curve for this model to the observed dispersion are shown in Figure 4. The average crustal structure beneath the profile consists of two layers (h_1 12 km, V_{s1} 3.65 km/s, h_2 23 km, V_{s2} 3.81 km/s) overlying a mantle with S_n velocity 4.61 km/s.

Receiver function analysis. Figures 5 and 6 illustrate the receiver function analysis we have performed using data from Bangalore (BGL). BGL is situated on the western edge of the eastern Dharwar craton close to its contact with the Closepet granitic intrusion (Figure 3). Figure 5 shows the BGL receiver function with respect to back azimuth. The eastern quadrant is well sampled, but there is only one event from the west. The small variation in the Ps converted phase (4.0±0.1) and the small amplitude of the tangential receiver function relative to the amplitude of the radial receiver function justify modeling the crust beneath BGL as 1-D.

Figure 6 (left) shows a receiver function stack for BGL consisting of 10 events with distance 76±7° and back azimuth 99±3° E. The receiver function has a large amplitude positive arrival at about 4 sec (PS) followed by a prominent positive arrival at about 14 seconds (PpP_mS) and a negative arrival at 16-18 seconds (PpS_mS + PSP_mS)). These phases are also apparent in many of the individual receiver functions making up the stack. Below the stack is the tangential receiver function. Amplitudes of the tangential arrivals are small compared to those of the radial arrivals.

The receiver function stack was inverted for 1-D crustal velocity models. To test the sensitivity of the inversion to the starting model, we used three different initial models: (1) the refraction model for the GBA region of Krishna and Ramesh (2000), (2) the average crustal model derived from the surface wave phase velocity dispersion (Figure 4), and (3) a model derived from the timing of the conversions and reverberations in the receiver functions and the average *P* wave velocity of the crust from Krishna and Ramesh (2000). Zandt *et al*. (1995) pointed out that the average crustal properties can be estimated directly from the arrival time differences of the pP, PS, PpP_mS and PpS_mS + PSP_mS phases in the receiver function. The PS - pP time difference is dependent on the average V_p/V_s ratio of the crust and the crustal thickness. The PS - PpP_mS time is the two-way *P* wave travel time and the {PpS_mS + PSP_mS} - pP time is the two-way *S* wave travel time through the crust for a ray with ray parameter *p*. The ratio of PS – pP to PS - PpP_mS is independent of crustal thickness but weakly dependent on V_p; the ratio of PS - PpP_mS to {PpS_mS + PSP_mS} is proportional to the V_p/V_s ratio and independent of crustal thickness.

We inverted the receiver functions using the linearized inversion of Ammon *et al.* (1990) both with and without the surface wave dispersion constraint and the final inversion results were nearly identical for the three starting models. We then simplified the model by grouping adjacent model layers with similar wave speeds to form a more coarsely parameterized starting model and reinverted the receiver function. We repeated this procedure until we found the velocity model with the minimum number of parameters that fit both the main features of the receiver function and the short period surface wave phase velocity. Finally, we tested the main features of the crustal model (e.g., thickness of the low velocity surface layer, thickness of the gradient at the base of the crust, Moho depth) using a forward-modeling model to estimate how well these model features were constrained by arrivals in the observed receiver function.

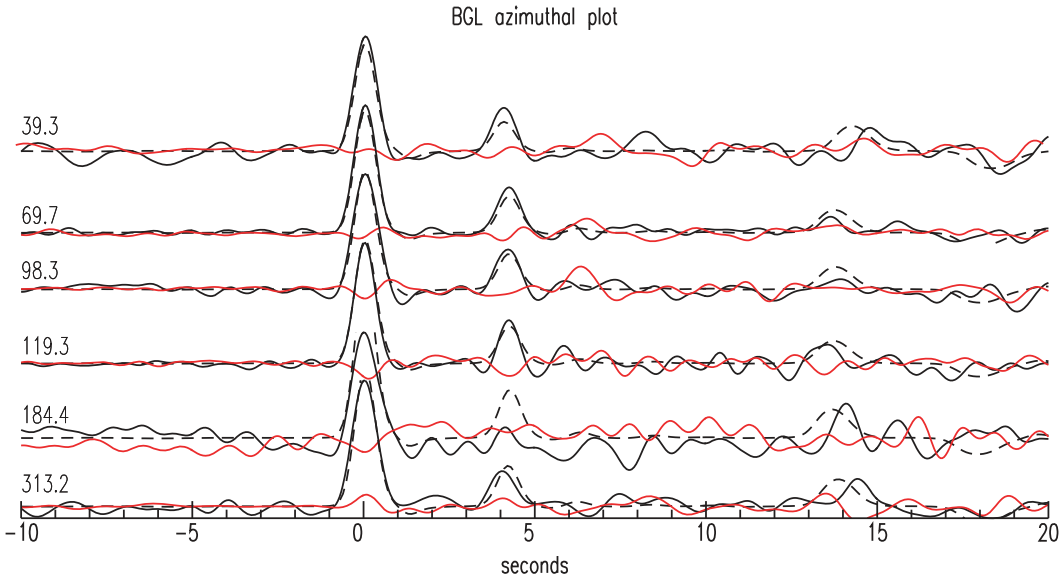

Figure 5. BGL receiver functions vs. azimuth: heavy solid line - radial receiver function; red solid line - tangential receiver function; dashed line - radial receiver function calculated for the final crustal velocity model shown in Figure 6.

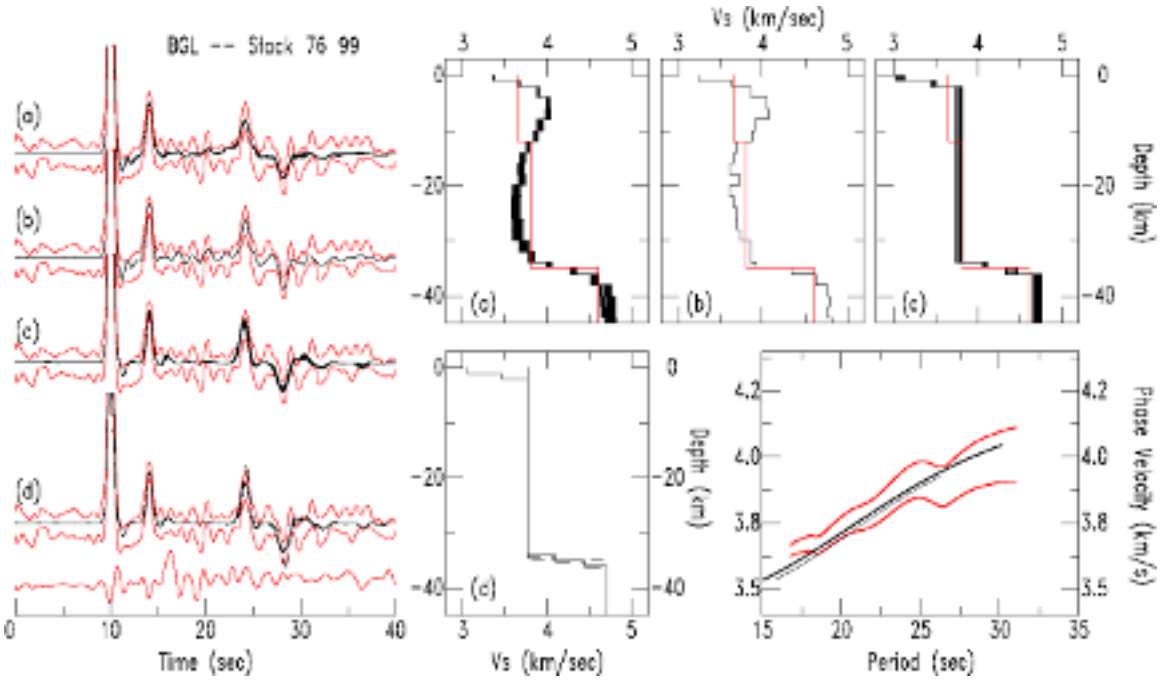

Figure 6. Receiver function analysis summary for BGL. Right: (a) initial inversion results; (b) results of joint receiver function/surface wave inversion; (c) final inversion models; (d) forward modeling test; (e) match between the observed phase velocity and the phase velocity calculated from the models shown in (b) and (c). Left: Match of the receiver function calculated for the four velocity models at right and the ±1 σ bounds for the BGL receiver function stack.

These steps are summarized in Figure 6 (right). The initial inversion model without the dispersion constraint shows a smooth velocity gradient from about V_s 3.1 km/s at the surface to about 3.75 km/s in the lower crust and a Moho discontinuity at 35±2 km depth (Figure 6a). The inversion with the surface wave dispersion constraint (Figure 6b) produces a model identical to those shown in Figure 6a. The final velocity model (Figure 6c) shows a thin (2-4 km) low velocity surface layer, an almost uniform velocity crust (3.5-3.6 km/s), and a Moho discontinuity at 35±1 km depth. The fits of the synthesized receiver functions for the various velocity models to the ±1σ bounds of the observed receiver function stack are shown in Figure 6 (left).

In the forward modeling test, the upper mantle *Pn* and *Sn* velocity were fixed at 8.2 km/s (Krishna and Ramesh, 2000) and 4.72 km/s (Huestis *et al*., 1973), respectively, but, in fact the receiver functions are relatively insensitive to these parameters. Neither the difference in the near surface layer, the mid-crustal discontinuity, nor the gradient at the base of the crust from the inversion of the different stacked receiver functions is significant, and we find that considering the noise in the data, one crustal velocity model fits all the receiver function stacks for BGL. Figure 5 compares the synthetic receiver function for the BGL crustal model which the observed receiver functions as a function of azimuth. This agreement indicates little lateral variation in the crustal velocity structure about BGL. If the small systematic variation in the PS - P time suggested by Figure 5 is real, this could result from a systematic variation of crustal velocity about BGL or a systematic variation in Moho depth. If the crustal velocity variation is spread through the whole 35 km thickness of the crust, it would correspond to a ±0.1 km/s variation in shear wave velocity. If the variation is due to a systematic azimuthal variation in the Moho depth, this corresponds to a ±1 km lateral variation in the Moho depth about BGL.

We have analyzed data from 14 broadband sites in southern India in this manner and the resulting Moho depths are shown in Figure 7. The Moho is at almost constant depth along the western edge of the eastern Dharwar craton. However, the two sites on the western Dharwar craton show the Moho there is about 5 km deeper, a result also noted in the Kavali - Uduppi refraction study (Kaila and Krishna, 1992). To the south of the shield in the granulite terrain (KOD, Fig. 1) the crust is 43 km thick. Thus, there are significant differences in Moho depth over southern India, but the results we have to date suggest they are well correlated with the surface geology.

Upper mantle structure beneath southern India. Figure 8 shows the fundamental mode Rayleigh waves dispersion measurement from seven two-station pairs using the combination of the stations NND/HYB in the north and GBA/KOD in the south. Inter-station path lengths for the two-station pairs vary from 600 to 800 km. The coherency plot shows that the dispersion is well constrained to ~180 sec period. Previous measurements of fundamental mode Rayleigh wave phase velocity have extended only to ~50 sec period (Hwang and Mitchell, 1987; Bhattacharya, 1992). This increased period range of our dispersion measurement is important in constraining the deep structure of the south Indian Shield. For comparison, the dispersion curve for the Canadian Shield (CANSD - Brune and Dorman, 1963) is also plotted in Figure 8. The crustal thickness of the south Indian Shield from the receiver function study discussed below is 36±1 km, and the crust of model CANSD is 35 km thick. The short period (<35 sec) and long period (>130 sec) portions of the two dispersion curves are similar, but between 40 and 125 sec period the phase velocities for the south Indian Shield are low compared to those of model CANSD. The preliminary inversion of the Indian phase velocity curves indicated the presence of a high velocity upper mantle lid with *S* wave velocity ranging from ~4.62 km/s at 40-60 km depth to ~4.72 km/s at 80-120 km depth and a low velocity of ~4.5 km/s at 150-220 km depth.

CONCLUSIONS AND RECOMMENDATIONS

During the past year, we have initiated a study to collect seismic data from southern Asia for the purpose of developing high quality velocity models to aid in regional seismic event location. We have installed five broadband sensors in southern Asia and are now collecting data. Using these data collected from the current deployment, along with other data sources from the region, we have completed surface wave and receiver function studies. Based upon surface wave phase velocity measurements, we have developed a shear wave velocity structure for the crust and upper mantle of the south Indian shield. The average crustal

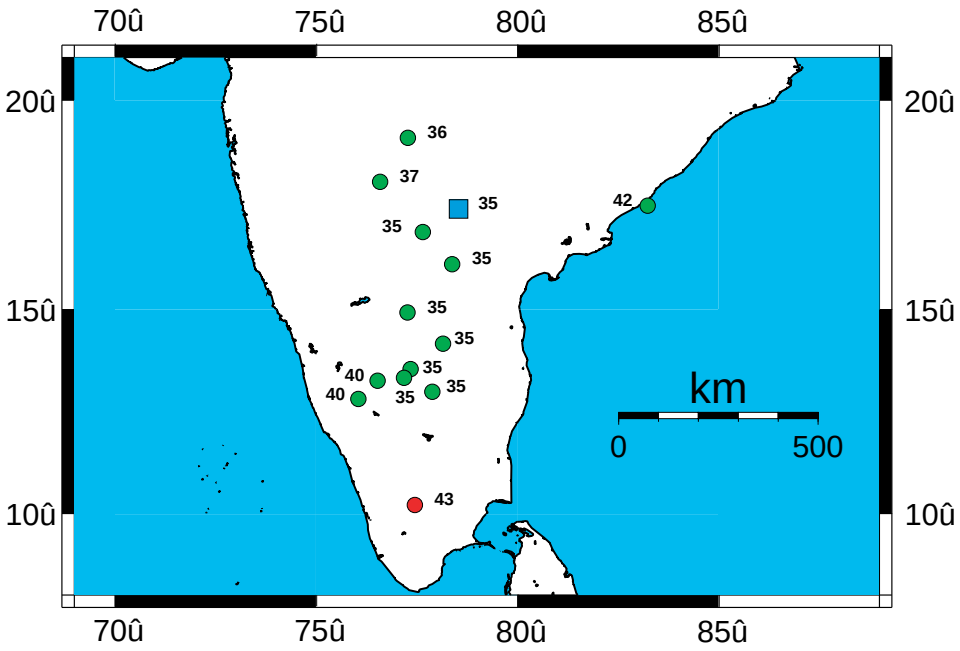

Figure 7. Moho depth from receiver function analysis.

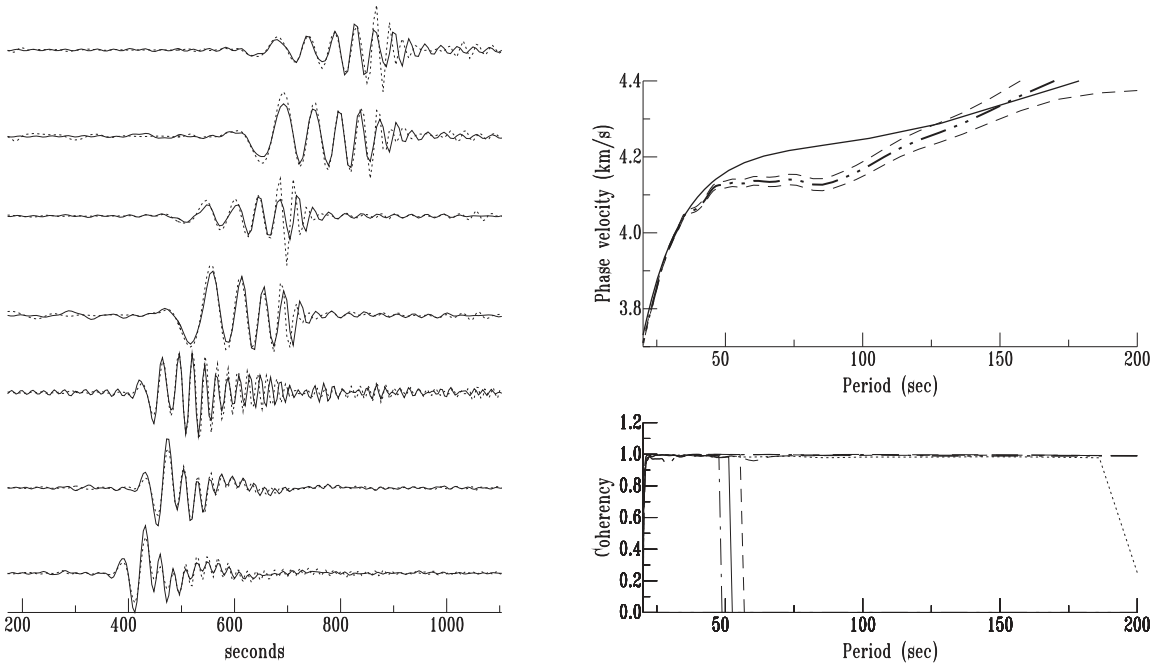

Figure 8. Long-period fundamental mode Rayleigh wave phase velocity dispersion. Left: Match of the far waveform (solid line) and near seismogram (dashed line) after being filtered by the determined transfer function. Right: Upper - dispersion curve for the south Indian Shield (dot-dash line) and ±1σ bounds (dash lines) and dispersion curve for model CANSD of Brune and Dorman (1963) (light solid line); Lower - coherency vs. period.

structure beneath the profile consists of two layers (h_1 12 km, V_{s1} 3.65 km/s, h_2 23 km, V_{s2} 3.81 km/s) overlying a mantle with S_n velocity 4.61 km/s. Inversions of the phase velocity curves indicate the presence of a high velocity upper mantle lid with *S* wave velocity ranging from ~4.62 km/s at 40-60 km depth to ~4.72 km/s at 80-120 km depth and a low velocity of ~4.5 km/s at 150-220 km depth. We have also analyzed receiver function data from 14 broadband sites in southern India and determine the velocity structure is similar to the surface wave results. The Moho is at almost constant depth along the western edge of the eastern Dharwar craton. However, the two sites on the western Dharwar craton show the Moho there is about 5 km deeper, a result also noted in the Deep Seismic Soundings from the region. To the south of the shield in the granulite terrain the crust is 43 km thick We have also modeled the regional waveforms of a moderate earthquake that occurred near Koyna, India, in September 2000 and of the 26 January 2001 Bhuj main shock and its aftershocks to calibrate paths to the regional stations. In the next stage of this project, we will continue the data collection and velocity model development, however our research focus will be shifted northward to central and eastern India, including the Shillong Plateau.

REFERENCES

Ammon, C.J., G.E. Randall and G. Zandt (1990), On the non-uniqueness of receiver function inversions. *J. geophys. Res.*, **95**, 15,303-15,318.

Bhattacharya, S.N. (1992), Crustal and upper mantle velocity structure of India from surface wave dispersion. In Gupta, H.K., S. Ramaseshan, (Eds.), Seismology in India - An Overview. *Curr. Sci.; Spec. Issue*, **62**, 94-100.

Brune, J.N., and J. Dorman (1963), Seismic waves and earth structure in the Canadian shield, *Bull. seism. Soc. Am.*, **53**, 167-210.

Du, Z.J., and G.R. Foulger (1999), The crustal structure of northwest fjords, Iceland, from receiver functions and surface waves, *Geophys. J Int.*, **139**, 419-432.

Gaur, V.K., and K.F. Priestley (1997), Shear wave velocity structure beneath the Archaean granites around Hyderabad, inferred from receiver function analysis, *Proc. Indian Acad. Sci. (Earth Planet. Sci.)*, **106**, 1-8.

Gomberg, J.S, K. Priestley, T.G. Masters, and J.N. Brune (1998), The Structure of the Crust and Upper Mantle of Northern Mexico, *Geophys. J. R. astr. Soc.*, **94**, 1-20.

Huestis, S., P. Molnar, and J. Oliver (1973), Regional *Sn* velocities and shear velocity in the upper mantle, *Bull. seism. Soc. Am.*, **63**, 469-475.

Johnson, M. B., S. Rieven, C. Vincent, D. Reiter, and W. Rodi (2000), Empirical analysis of a 3-D Pakistan regionalized velocity model for improved seismic event locations, Proceedings of the 22nd Annual DoD/DOE Seismic Researh Symposium, 43-52.

Hwang, H. G., and B. J. Mitchell (1987), Shear velocities, Q_β, and the frequency dependence of Q_β in stable and tectonically active regions from surface wave observations, *Geophys. J. R. astr. Soc.*, **90**, 575-613.

Kaila, K.L., and V.G. Krishna (1992), Deep seismic sounding studies in India and major discoveries. In Gupta, H.K., S. Ramaseshan, (Eds.), Seismology in India - An Overview. *Curr. Sci.; Spec. Issue*, **62**, 117-154.

Krishna, V.G., C.V.R.K. Rao, H.K. Gupta, D. Sarkar, and Baumbach (1999), Crustal seismic velocity structure in the epicentral region of the Latur earthquake (September 29, 1993), southern India: inferences from modeling of the aftershock seismograms, *Tectonophysics*, **304**, 241-255.

Krishna, V.G., and D.S. Ramesh (2000), Propagation of crustal waveguide trapped Pg and seismic velocity structure in the south Indian shield, *Bull. seism. Soc. Am.*, **90**.

Mandal, P., B. K. Rastogi, and C. S. P. Sarma (1998), Source parameters for Koyna earthquakes, India, *Bull. seism. Soc. Am.*, **88**, 833-842..

Singh, S.K., R.S. Dattatrayam, N.M. Shapiro, P. Mandal, J.F. Pacheco, and R.K. Midha (1999), Crustal and Upper Mantle structure of peninsular India and source parameters of the 21 May 1997, Jabalpur earthquake (Mw = 5,8): Results from the new regional broadband network, *Bull. seism. Soc. Am.*, **89**, 1631-1641.